# *Ab initio* configuration interaction calculations of the predissociation of rovibrational levels of the $C\ ^3\Pi_g$ and $d\ ^1\Pi_g\ 3s\sigma$ Rydberg states of the oxygen molecule

Yan Li, Ioannis D. Petsalakis,[a] Heinz-Peter Liebermann, Gerhard Hirsch, and Robert J. Buenker
*Bergische Universität, Gesamthochschule Wuppertal, Fachbereich 9, Theoretische Chemie, Gaußstr. 20, D-42097 Wuppertal, Germany*

(Received 29 May 1996; accepted 8 October 1996)

*Ab initio* configuration interaction calculations have been carried out for seven low-lying $^{3,1}\Pi_g$ states of the oxygen molecule. Three different types of nonadiabatic couplings have been considered: spin-orbit, radial, and rotational. The complex scaling method has been employed to compute rovibrational level locations and predissociation linewidths with a basis of 200 Hermite polynomials for each of 13 different $\Omega$ electronic states. The calculations correctly predict that the $v=2$ level has the narrowest linewidth for the $^{16}O_2$ $C\ ^3\Pi_g$ state, while $v=4$ is narrowest for $^{18}O_2$. Marked variations in the linewidths of the different $\Omega$ components of the $C$ state are explained by the fact that the $\pi^*\rightarrow 3s\sigma$ Rydberg and $\sigma\rightarrow\pi^*$ valence $^3\Pi_g$ states have different occupations of the $\pi^*$ orbital, causing opposite orderings of their respective $\Omega$ levels. Rotational coupling is found to be important for high $J$ values of the $C$ state. The $d\ ^1\Pi_g\ 3s\sigma$ state shows even more unusual effects by virtue of the fact that there is a sharply avoided crossing between the corresponding Rydberg diabatic state with a bound $\sigma\rightarrow\pi^*\ ^1\Pi_g$ valence state. The calculations find irregular spacings in the $d$-state vibrational manifold, wide variations in linewidth for different $v,J$ levels, and a large change in the rotational constant in successive vibrational levels, all of which effects have been earlier demonstrated in experimental work. Satellite lines are indicated for both the $v=2$ and 3 levels as a result of the interaction with the bound $^1\Pi_g$ valence state, whereby experimental verification exists only for $v=2$. The $v=3$ state has not yet been successfully identified due to the broadness of the $d$-$X$ spectrum in the energy range of interest. The observed temperature dependence of the linewidths of the two features near the expected location of the $v=2$ level can also be understood on the basis of these calculations. Finally, the change in the predissociation mechanism for the $d$ state from spin-orbit to radial as $v$ changes from 0 to 2 which has been deduced experimentally is also verified in the present theoretical treatment. [S0021-9606(97)01303-2]

## I. INTRODUCTION

The $C\ ^3\Pi_g(3s\sigma)$ and $d\ ^1\Pi_g(3s\sigma)$ Rydberg states of the oxygen molecule have attracted great interest in the last decade because of their unusual spectroscopic properties.[1–15] York *et al.*[1] identified the first four vibrational levels of the $C$ state by analyzing their electron energy-loss spectrum (EELS), while Sur *et al.*[2] characterized the first five vibrational levels of the $d$ state using (2+1) resonance enhanced multiphoton ionization spectroscopy (REMPI). In the latter study, a rotational constant $B_0$ of 1.68 $cm^{-1}$ was determined. At about the same time, Sur *et al.*[3] also reported optical spectra involving the $^3\Pi_g(3s\sigma)$ state. They noted that among the first five vibrational levels only $v=2$ exhibits rotationally resolved structure, and also that the corresponding three spin components have significantly different linewidths. Katsumata *et al.*[4] also studied the $C$ $v=2$ level by analysis of their MPI ion-current and photoelectron spectra. They reported spin splittings of 84 and 106 $cm^{-1}$ for $F_2$-$F_1$ and $F_3$-$F_2$, respectively.

On the basis of a resonance enhanced multiphoton ionization (REMPI) spectrum of the $O_2$ $a\ ^1\Delta_g$ state between 305 and 350 nm, Johnson *et al.*[5] were able to identify the $v=0$–3 levels of the $d\ ^1\Pi_g(3s\sigma)$ upper state. The rotational constant for the $v'=3$ level was determined to be 1.167 $cm^{-1}$, notably smaller than that found for the corresponding $v=3$ of the $X\ ^2\Pi$ state of $O_2^+$, and this observation was later confirmed by Sur *et al.*[9] Van der Zande *et al.*[6–8] employed translational spectroscopy to investigate the $v=0$–2 and 4–7 vibrational levels of the $d$ state, as well as for $v=0$–2 of the $C$ state. The energy locations of all of these levels were measured, as well as linewidths for the $v=4$–7, $J=1$–25 rovibrational levels of the $d$ state. The same authors[8] also investigated the predissociation of the $v=0$–2 levels of the $d$ state and concluded that a spin-orbit coupling mechanism involving the lower $C$ state is predominantly responsible for the observed $v=0$ line broadening. They also determined the 0–0 and 1–1 energy spacings between these two Rydberg excited states. More recently, Sur

[a]On leave from the Theoretical and Physical Chemistry Institute, National Hellenic Research Foundation, 48, Vas Constantinou Avenue, GR-11635 Athens, Greece.

*et al.*[10] obtained linewidth data for several $O_2$ isotopomers in low vibrational levels of the $C$ state. They found that for $^{16}O_2$ the $v=2$ level is the narrowest among the $v=0-4$ species, while in the case of $^{18}O_2$ the $v=4$ linewidth is smaller than that of $v=2$.

On the theoretical side, van der Zande *et al.*[7] have empirically deduced the magnitude of the nonadiabatic coupling matrix element between the $^1\Pi_g(3s\sigma)$ Rydberg and the bound $^1\Pi_g$ valence states based on the Fermi golden rule. They adapted the RKR curve of the $X\ ^2\Pi_g\ O_2^+$ ground state as the Rydberg potential curve and adjusted the *ab initio* data of Saxon and Liu[16–18] for the corresponding $^1\Pi_g$ valence curve, and assumed a distance-independent coupling matrix element. Van der Zande *et al.*[8] have determined the coupling between the 1 and $2\,^1\Pi_g$ valence states based on the Landau–Zener formula by adjusting the coupling to fit the measured transition probability. These authors also carried out calculations for the predissociation of the $v=0-2$ levels of the $d$ state. For this purpose the measured spin-orbit splittings for the three components of the $C\ ^3\Pi_g(3s\sigma)$ state were employed, as well as the experimental $d$-$C$ energy spacing. Friedman *et al.*[12] employed the above potential curves in coupled differential equations which were integrated numerically to compute rotational constants for the $v=0-4$ levels of the $d\ ^1\Pi_g$ state. They also solved coupled scattering equations based on an empirical $2\,^3\Pi_g$ valence state potential curve and adjusted nonadiabatic matrix elements to reproduce the observed level positions and linewidths for the $C\ ^3\Pi_g\ v=0-4$ states.[13,14] Sur *et al.*[10] calculated isotopic shifts in the same vibrational states by employing the Fermi golden rule with trial potential curves and an empirical $r$-independent nonadiabatic coupling constant. In our laboratory *ab initio* CI calculations were carried out for the $^3\Pi_g(3s\sigma)$, $^3\Pi_g(4s\sigma)$, and $^3\Pi_g(\sigma\rightarrow\pi^*)$ states and diabatic potential curves and $r$-dependent nonadiabatic matrix elements were constructed.[15] By applying the complex scaling method[19–23] to these theoretical results it was possible to compute level positions and linewidths for the $v=0-4$ vibrational states of $C\ ^3\Pi_g$, and these results were found to be in reasonably good agreement with the observed data.

Up to the present, however, there has been little theoretical work dealing with the dramatic changes in the linewidths between different $\Omega$ components of a given $C\ ^3\Pi_g$ rovibrational level, such as for $v=2$, for example. There also have been no *ab initio* calculations of the spin-orbit splitting of the $^3\Pi_g(3s\sigma)$ Rydberg state and its interaction with the nearby $d\ ^1\Pi_g$ state of $O_2$. Furthermore, no theoretical investigation has concerned itself with the effects of the interaction between rotational and electronic angular momentum on these line positions and widths. In the present study we present an *ab initio* treatment of the various $O_2\ ^{3,1}\Pi_g$ potential curves, as well as the spin-orbit, radial, and rotational coupling matrix elements between them. These data are obtained with highly correlated multireference configuration interaction (MRD-CI) wave functions and are subsequently employed in the framework of the complex scaling technique to obtain the energy locations and linewidths of the $v=0-7$, $J=1-25$ levels of the $d\ ^1\Pi_g(3s\sigma)$ and the $v=0-5$, $J=1-25$ levels of the corresponding triplet Rydberg state $C$.

## II. DETAILS OF THE CALCULATIONS

Since spin-orbit coupling is a key interaction in the present discussion, it was decided to carry out the calculations with the aid of effective core potentials (ECP) which are specifically derived to compute this type of matrix element. The ECP of Christiansen *et al.*[24] is employed to describe the oxygen atom, so that only its $2s$ and $2p$ electrons need to be considered explicitly in the *ab initio* CI treatment. Their $(4s4p)$ AO basis is employed without contraction in the present calculations, augmented by $d$-type polarization and Rydberg-type $s$ and $p$ functions. The exponents for the $d$ functions have been specifically optimized for this purpose, with values of 0.70 and 2.35 (all six Cartesian components are retained in each case). The Rydberg exponents are taken from the work of Dunning and Hay.[25] The effects of adding an $f$ function to the AO basis have been studied in earlier work.[20] The ground state vibrational frequency was increased by 12.5 $cm^{-1}$, for example, bringing it to within 11.1 $cm^{-1}$ of the measured value. Especially since some refinement of the computed results is found to be necessary to obtain suitable spacings of the various potential curves of interest in the present study, it was decided that the addition of $f$ and higher-order spherical harmonics to the AO basis would not justify the greater computational expenses this would imply.

Restricted open-shell Hartree–Fock calculations with this AO basis have been carried out for the $X\ ^3\Sigma_g^-O_2$ ground state at each of a large series of internuclear distances between $r=1.82$ and 9.00 $a_0$, and the resulting MOs form the one-electron basis in a subsequent multireference single- and double-excitation configuration interaction (MRD-CI) treatment[26–28] for the excited $^{3,1}\Pi_g$ electronic states of interest in the present work. The number of reference configurations employed for the $^3\Pi_g$ calculations is 25, and the configuration selection is based on results for the lowest three roots of this symmetry. For the $^1\Pi_g$ states 60 reference configurations have been chosen, and in this case the first four roots are considered in the selection process. Employing a threshold of $T=0.2\ \mu E_h$ leads to secular equations of ca. 80 000 on the average for each multiplicity. Some tests were made with lower selection threshold, but it was found that the larger secular equations which result do not have a significant effect on the locations of the computed vibrational levels, indicating that a suitable degree of convergence has been achieved in the present CI treatment. A direct CI procedure recently implemented in our laboratory[29] was employed to obtain the desired eigenvalues and eigenvectors. The computation of the Hamiltonian matrix elements themselves is done with the help of the Table CI algorithm described elsewhere.[30] The standard MRD-CI perturbative techniques are then applied to account for the effects of unselected singly and doubly excited configurations on the energy eigenvalues, and the multireference analogue of the Davidson correction[31,32] is also employed to estimate the contribution of more highly excited configurations (esti-

mated full-CI energy values). As in an earlier study[15] of the $O_2$ $^3\Pi_g$ states, the calculations are formally carried out in $D_{2h}$ symmetry, although the MOs themselves do transform according to the irreducible representations of the full $D_{\infty h}$ point group.

The three $^3\Pi_g$ adiabatic states obtained in the CI calculations are mixtures of the $1\pi_g \rightarrow 3s\sigma, 1\pi_g \rightarrow 4s\sigma$, and $3\sigma_g \rightarrow 1\pi_g$ diabatic states. At each internuclear distance a unitary transformation of the adiabatic wave functions is effected by diagonalizing the $x^2+y^2$ quadrupole moment property. A similar procedure was carried out for the corresponding singlet states. This technique works quite well because the diabatic states in question can be distinguished quite easily on the basis of this property.[20] In the case of the $^1\Pi_g$ states, it was necessary to carry out an additional transformation of the two valence states resulting from the $3\sigma_g \rightarrow 1\pi_g$ and $1\pi_u \rightarrow 3\sigma_u$ excitations, respectively, by assuming that the off-diagonal Hamiltonian matrix element in the diabatic representation is the same at all internuclear distances.

The same set of (diabatic) transformations was applied to the adiabatic spin-orbit matrix formed on the basis of six of the above $^{3,1}\Pi_g$ states. It was found that matrix elements between Rydberg and valence $\Pi_g$ diabatic states are of negligible magnitude ($<1.0\times10^{-5}E_h$) in each case, as one should expect for such a relatively light system, thus verifying the adequacy of the transformation employed and supporting its transferability from the $\lambda$-$s$ to the $\Omega$ space. A matrix representation of the electronic Hamiltonian including the spin-orbit operator is then formed in the diabatic basis to obtain the $\Omega=0^{\pm}$,1,2 components of the $^3\Pi_g$ $\lambda$-$s$ states. It was invariably found that the order of the three spin components for the valence $^3\Pi_g$ state is inverted relative to that of the two Rydberg species, namely $\Omega(0)<\Omega(1)<\Omega(2)$ for Rydberg and the opposite for valence. This finding is critical for understanding the large distinction in the observed linewidths of the three spin components of the $^3\Pi_g(3s\sigma)$ Rydberg state. In addition the $J\cdot S$ (heterogeneous $S$-uncoupling) perturbation has been computed according to the formula[33]

$$\begin{aligned}\langle \Lambda,S,\Sigma,\Omega,v|-(2\mu R^2)^{-1}J^{\pm}S^{\mp}|\Lambda,S,\Sigma\pm1,\Omega\pm1,v'\rangle \\ =\langle v|-(2\mu R^2)^{-1}|v'\rangle[S(S+1)-\Sigma(\Sigma\pm1)]^{1/2} \\ \times[J(J+1)-\Omega(\Omega\pm1)]^{1/2}. \qquad (1)\end{aligned}$$

The selection rules which must be obeyed are

$$\Delta J=0,\ \Delta P=0,\ \Delta\Omega=\pm1,\ \Delta S=0,\quad \Delta\Lambda=0,$$

and

$$\Delta\Sigma=\pm1. \qquad (2)$$

The three $^3\Pi_g$ and four $^1\Pi_g$ states considered contain 26 multiplets in all. When combined with rotational functions of a given $J$, it is possible to divide the resulting product wave functions strictly into two classes according to their respective parities. The $0^+$ and $0^-$ functions always differ in this property and couple with different $\Lambda$-doubled components of the $\Omega=1,2$ states. In forming the rovibrational Hamiltonian matrices it is possible to take full advantage of this separation. For a given $J$ value each electronic function is multiplied with 200 Hermite polynomials. After coupling with the rotational functions of a given $J$, 13 species of $+$ symmetry and 13 of $-$ result for each vibrational function. Two secular equations of $200\times13=2600$ order result which are exactly the same and thus only a single diagonalization is required to obtain the desired rovibronic energy eigenvalues. In the present calculations no states with $\Lambda\neq1$ are included, which appears to be a suitable approximation for the application at hand. Hence, there is no splitting between the two $\Lambda$ rotational components in any case, including the respective $0^+$ and $0^-$ electronic states corresponding to the same configuration, and equal rovibronic Hamiltonian matrices arise as a result.

The various diabatic potential energy curves and off-diagonal electronic Hamiltonian matrix elements, including the spin-orbit results, are first fitted to polynomials before computing the rovibronic Hamiltonian matrix numerically.[19] More details of this phase of the calculations may be found in our earlier study of the $O_2$ $^3\Pi_g$, $^3\Sigma_g^-$ states.[15,20] The complex scaling technique is then applied to this matrix in order to compute the energy locations and linewidths of the resonance states of interest. As found in the earlier study,[20] the use of a relatively large basis of Hermite polynomials for each electronic state is very important for obtaining numerically stable complex eigenvalues. For the $r\rightarrow re^{i\Theta}$ scaling it was found that both the real and imaginary parts of the complex energy eigenvalue were very nearly constant for a fairly large range of $\Theta$ centered around $8^0$, so that resonance states could be unambiguously identified in all cases. In order to obtain the best possible agreement with experimental results for the $^{3,1}\Pi_g(3s\sigma)$ rovibrational linewidth data, it was necessary to alter the potential curves of the nearby $^{3,1}\Pi_g$ valence states. The bound $^1\Pi_g$ valence state potential curve was first shifted upward by 1100 $cm^{-1}$ so that the difference between its asymptotic energy ($^1D+{}^1D$) and the computed location of the $C$ $^3\Pi_g$ $v=0$ state agrees with the corresponding measured value. This curve was then moved to a smaller internuclear distance by 0.038 $a_0$ in order that the originally computed location of the crossing with the Rydberg potential curve be unchanged. The corresponding $^3\Pi_g$ valence state was also displaced to smaller $R$ values, but by only 0.008 $a_0$. No energy shift was found to be desirable for this state, however, and all other potential curves and coupling elements were taken without change from the *ab initio* CI calculations. This level of accuracy for the relative spacings of the computed potential energy curves is quite typical for MRD-CI calculations with the present type of AO basis.

## III. DISCUSSION OF RESULTS

### A. Potential curves and matrix elements

The CI potential energy curves calculated for the four $^1\Pi_g$ and three $^3\Pi_g$ low-lying Rydberg and valence states of $O_2$ are shown in Fig. 1 and the corresponding total energy values are given in Table I. The $\pi^*\rightarrow3s\sigma$, $4s\sigma$ $^{3,1}\Pi_g$ Rydberg states have potential minima for $r$ values less than the $X$ $^3\Sigma_g^-$ ground state equilibrium distance, reflecting the

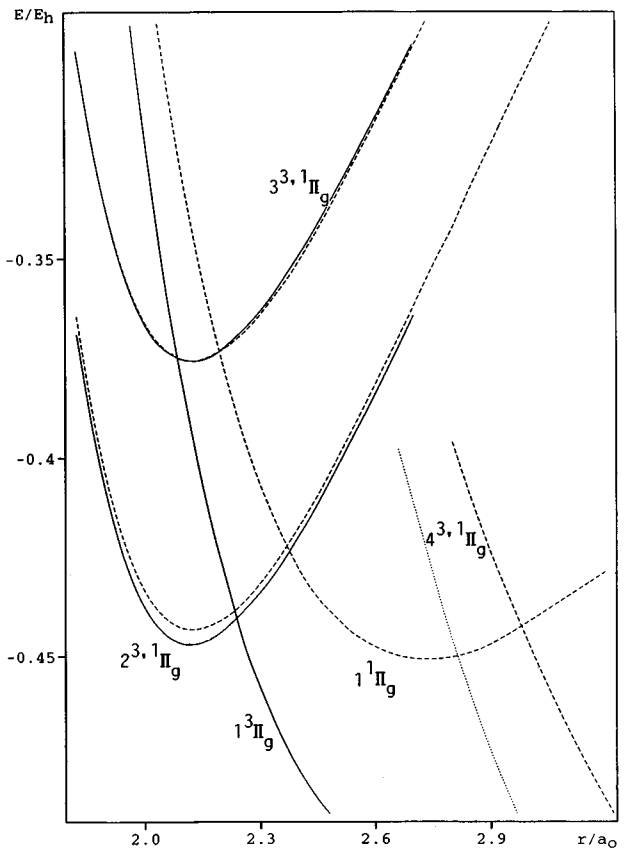


FIG. 1. Computed diabatic potential energy curves of various $^3\Pi_g$ (solid lines) and $^1\Pi g$ (dashed lines) states of the $O_2$ molecule. The estimated location of the $4\,^3\Pi_g$ state is indicated by a dotted curve.

antibonding nature of the $\pi^*$ MO. The triplet–singlet splittings are relatively small, especially for the $^{3,1}\Pi_g(4s\sigma)$ pair. The $\sigma\rightarrow\pi^*$ $^3\Pi_g$ potential cuts through the $^{3,1}\Pi_g(3s\sigma)$ (diabatic) counterparts just to the long-distance side of their respective minima (Fig. 1). The corresponding $^1\Pi_g$ valence state lies about 1 eV above the $\sigma\rightarrow\pi^*$ $^3\Pi_g$, and so its potential curve cuts through the $^{3,1}\Pi_g(3s\sigma)$ potentials at much higher energy. It has a pronounced minimum near $r=2.73$ $a_0$, unlike the triplet state. There is another pair of valence $\Pi_g$ states in the general area. They arise in the main from a $\pi\rightarrow\sigma^*$ excitation and thus are strongly repulsive. The $\pi\rightarrow\sigma^*$ singlet potential curve has been calculated explicitly in this work because it has an important curve crossing with the $\sigma\rightarrow\pi^*$ state of the same multiplicity, but the corresponding triplet state results are simply estimated in Fig. 1, since this state plays no role in the interactions of interest. Only the diabatic potentials are shown in the figure since they do not differ greatly from the untransformed adiabatic CI results except in the immediate area of avoided crossings. Similarly, the effects of spin-orbit coupling are neglected at this stage of the calculations, since the corresponding matrix elements are relatively small for such a light system. The radial nonadiabatic couplings between the $\pi\rightarrow\sigma^*$ $^1\Pi_g$ state and the two Rydberg species ($E_{24}$ and $E_{34}$) have simply been assumed to be of vanishing magnitude, whereas that between the two valence $^1\Pi_g$ states ($E_{14}$) is taken to be independent of $r$, as already discussed in Sec. II. The couplings between the other diabatic states are shown in Table I as a function of internuclear distance. For this purpose the following labeling scheme has been adopted for both the $^{3,1}\Pi_g$ sets of states: $\sigma\rightarrow\pi^*$ (1), $\pi^*\rightarrow 3s\sigma$ (2), $\pi^*\rightarrow 4s\sigma$ (3), and $\pi\rightarrow\sigma^*$ (4). The coupling between the lowest Rydberg and valence states ($E_{12}$) is fairly strongly $r$-dependent for both multiplicities, and is somewhat larger for the singlet pair. The $E_{13}$ matrix elements also vary with $r$, but are only 10%–20% as large, reflecting the more diffuse character of the $4s\sigma$ MO.

The calculated spin-orbit matrix elements are given in Table II for different $x,y$ components of the same diabatic triplet state and for corresponding singlet/triplet states, respectively. As mentioned in Sec. II, the couplings between diabatic Rydberg and valence states are found to be less than $1.0\times10^{-5}E_h$ in each case, and thus have been neglected in the treatment of nuclear motion to be discussed below. Such small values are expected for the interaction of *pure* Rydberg and valence states, and thus amount to a verification of the effectiveness of the diabatization procedure employed in the present work. The spin-orbit couplings in Table II are seen to fall in the $0.3–0.4\times10^{-3}E_h$ range for each pair of functions at every $r$ value considered. In other words, they are not greatly different for Rydberg and valence states. This can be understood on the basis of the fact that in all cases it is the same ($\pi^*$) MO which is primarily responsible for the effect. One important distinction can be seen in Table IIa, however, namely that the sign of the $\sigma\rightarrow\pi^*$ $^3\Pi_g$ matrix element $<1|SO|1>$ is opposite to that of the corresponding Rydberg $(3s\sigma)$ value. This is a typical inversion phenomenon caused by the fact that the $\pi^*$ MO is triply occupied in the $\sigma\rightarrow\pi^*$ valence state, whereas it is only singly occupied in the $\pi^*\rightarrow 3s\sigma$ Rydberg state. As mentioned in Sec. II, the $^3\Pi_g$ $\Omega$ components have a different order for Rydberg and valence states and this is directly related to the above difference in signs in their respective $x,y$ matrix elements.

### B. Linewidths and energy locations

The energy positions and linewidths of the $v=0–5/J=2–25$ levels of the $C\,^3\Pi_g(3s\sigma)$ state have been computed for both the $^{16}O_2$ and $^{18}O_2$ isotopomers, and these results are summarized in Table III. The analogous data for the $v=0–7/J=1–25$ levels of the $d\,^1\Pi_g(3s\sigma)$ state are given in Table IV. The energy spacing between the $v=0$ levels of these two states is computed to be 649 $cm^{-1}$ for $J=1$ and 643 $cm^{-1}$ for $J=25$. The corresponding observed $T_{00}$ value[9,10] is 699 $cm^{-1}$, so the computed values are too low by about 7%. The theoretical $C$-$X$ $T_{00}$ value itself is 65 698 $cm^{-1}$, which is in excellent agreement with the measured value of 65 681 $cm^{-1}$($^{16}O_2$).

Because of the spin-orbit interaction each rotational level of the $C\,^3\Pi_g$ state with $J>1$ is split into three components, $F_1$-$F_3$. For $v=0$, $J=2$, for example, $F_1$ is found to lie 79 $cm^{-1}$ below $F_2$ and $F_3$ 97 $cm^{-1}$ above it (Table III). For $v=2$ the corresponding values are 74 and 98 $cm^{-1}$ for $J=2$ and 85 and 108 $cm^{-1}$ for $J=25$. These

TABLE I. Calculated diabatic potential energies $E_{ii}$ of the $^{3,1}\Pi_g$ states of $O_2$ studied, together with the respective nondiagonal energies $E_{ij}$ (in $E_h$) as function of the bond distance $r$ (in $a_0$).

| $r$ | $E_{11}$(val) | $E_{22}$ (Ryd) | $E_{33}$ (Ryd) | $E_{44}$(val) | $E_{12}$ | $E_{13}$ | $E_{23}$ |
|---|---|---|---|---|---|---|---|
| | | | $^3\Pi_g$ potentials[a] | | | | |
| 1.820 | −1.144 261 | −1.368 697 | −1.297 809 | | 0.008 770 | 0.001 714 | 0.018 493 |
| 1.860 | −1.193 771 | −1.392 013 | −1.320 857 | | 0.007 541 | 0.001 786 | 0.018 529 |
| 1.900 | −1.237 295 | −1.410 179 | −1.338 854 | | 0.006 727 | 0.001 713 | 0.018 535 |
| 1.940 | −1.275 501 | −1.423 917 | −1.352 511 | | 0.006 189 | 0.001 551 | 0.018 522 |
| 1.980 | −1.308 987 | −1.433 876 | −1.362 465 | | 0.005 817 | 0.001 346 | 0.018 497 |
| 2.020 | −1.338 286 | −1.440 635 | −1.369 280 | | 0.005 528 | 0.001 130 | 0.018 469 |
| 2.040 | −1.351 517 | −1.442 975 | −1.371 667 | | 0.005 396 | 0.001 027 | 0.018 455 |
| 2.060 | −1.363 876 | −1.444 702 | −1.373 452 | | 0.005 265 | 0.000 930 | 0.018 441 |
| 2.080 | −1.375 415 | −1.445 869 | −1.374 685 | | 0.005 132 | 0.000 840 | 0.018 430 |
| 2.100 | −1.386 182 | −1.446 527 | −1.375 415 | | 0.004 992 | 0.000 759 | 0.018 420 |
| 2.120 | −1.396 221 | −1.446 722 | −1.375 688 | | 0.004 846 | 0.000 688 | 0.018 412 |
| 2.140 | −1.405 576 | −1.446 497 | −1.375 546 | | 0.004 691 | 0.000 627 | 0.018 407 |
| 2.160 | −1.414 287 | −1.445 894 | −1.375 027 | | 0.004 527 | 0.000 576 | 0.018 405 |
| 2.180 | −1.422 397 | −1.444 948 | −1.374 167 | | 0.004 356 | 0.000 535 | 0.018 405 |
| 2.200 | −1.429 923 | −1.443 694 | −1.372 998 | | 0.004 179 | 0.000 504 | 0.018 408 |
| 2.220 | −1.436 916 | −1.442 163 | −1.371 551 | | 0.003 997 | 0.000 481 | 0.018 414 |
| 2.240 | −1.443 400 | −1.440 383 | −1.369 852 | | 0.003 812 | 0.000 461 | 0.018 423 |
| 2.260 | −1.449 406 | −1.438 379 | −1.367 927 | | 0.003 628 | 0.000 458 | 0.018 435 |
| 2.280 | −1.454 958 | −1.436 175 | −1.365 798 | | 0.003 446 | 0.000 456 | 0.018 450 |
| 2.300 | −1.460 084 | −1.433 791 | −1.363 485 | | 0.003 270 | 0.000 458 | 0.018 467 |
| 2.320 | −1.464 807 | −1.431 249 | −1.361 006 | | 0.003 103 | 0.000 462 | 0.018 487 |
| 2.340 | −1.469 149 | −1.428 556 | −1.358 377 | | 0.002 946 | 0.000 469 | 0.018 509 |
| 2.360 | −1.473 131 | −1.425 733 | −1.355 613 | | 0.002 803 | 0.000 475 | 0.018 534 |
| 2.380 | −1.476 773 | −1.422 793 | −1.352 727 | | 0.002 675 | 0.000 480 | 0.018 560 |
| 2.400 | −1.480 095 | −1.419 744 | −1.349 730 | | 0.002 565 | 0.000 484 | 0.018 588 |
| 2.420 | −1.483 115 | −1.416 597 | −1.346 631 | | 0.002 473 | 0.000 483 | 0.018 618 |
| 2.460 | −1.488 318 | −1.410 033 | −1.340 164 | | 0.002 348 | 0.000 470 | 0.018 680 |
| 2.500 | −1.492 517 | −1.403 144 | −1.333 382 | | 0.002 294 | 0.000 437 | 0.018 746 |
| 2.540 | −1.495 842 | −1.395 956 | −1.326 332 | | 0.002 294 | 0.000 385 | 0.018 814 |
| 2.580 | −1.498 422 | −1.388 480 | −1.319 043 | | 0.002 309 | 0.000 319 | 0.018 883 |
| 2.620 | −1.500 394 | −1.380 719 | −1.311 566 | | 0.002 283 | 0.000 254 | 0.018 951 |
| 2.640 | −1.501 195 | −1.376 730 | −1.307 761 | | 0.002 228 | 0.000 228 | 0.018 985 |
| 2.700 | −1.503 095 | −1.364 321 | −1.296 144 | | 0.001 742 | 0.000 223 | 0.019 086 |
| 2.750 | −1.557 475 | −1.354 511 | −1.286 490 | | 0.001 600 | 0.000 190 | 0.019 173 |
| 2.800 | −1.580 756 | −1.344 394 | −1.276 860 | | 0.001 500 | 0.000 160 | 0.019 268 |
| | | | $^1\Pi_g$ potentials [a] | | | | |
| 1.82 | −1.120 564 | −1.364 561 | −1.298 796 | | 0.010 992 | 0.002 803 | 0.019 489 |
| 1.86 | −1.165 644 | −1.387 658 | −1.320 326 | | 0.010 076 | 0.002 469 | 0.019 418 |
| 1.90 | −1.205 599 | −1.405 701 | −1.337 741 | | 0.009 229 | 0.002 167 | 0.019 361 |
| 1.94 | −1.240 903 | −1.419 430 | −1.351 400 | | 0.008 448 | 0.001 897 | 0.019 315 |
| 1.98 | −1.271 996 | −1.429 491 | −1.361 672 | | 0.007 728 | 0.001 656 | 0.019 280 |
| 2.02 | −1.299 283 | −1.436 450 | −1.368 928 | | 0.007 066 | 0.001 442 | 0.019 256 |
| 2.04 | −1.311 616 | −1.438 921 | −1.371 541 | | 0.006 755 | 0.001 344 | 0.019 247 |
| 2.06 | −1.323 136 | −1.440 793 | −1.373 538 | | 0.006 458 | 0.001 253 | 0.019 241 |
| 2.08 | −1.333 882 | −1.442 118 | −1.374 962 | | 0.006 174 | 0.001 167 | 0.019 236 |
| 2.10 | −1.343 897 | −1.442 941 | −1.375 856 | | 0.005 902 | 0.001 086 | 0.019 234 |
| 2.12 | −1.353 217 | −1.443 306 | −1.376 263 | | 0.005 643 | 0.001 011 | 0.019 234 |
| 2.14 | −1.361 881 | −1.443 253 | −1.376 222 | | 0.005 395 | 0.000 941 | 0.019 235 |
| 2.16 | −1.369 922 | −1.442 817 | −1.375 773 | | 0.005 159 | 0.000 875 | 0.019 239 |
| 2.18 | −1.377 376 | −1.442 033 | −1.374 953 | | 0.004 933 | 0.000 814 | 0.019 244 |
| 2.20 | −1.384 273 | −1.440 932 | −1.373 797 | | 0.004 718 | 0.000 758 | 0.019 250 |
| 2.22 | −1.390 646 | −1.439 541 | −1.372 839 | | 0.004 514 | 0.000 705 | 0.019 259 |
| 2.24 | −1.396 523 | −1.437 886 | −1.370 610 | | 0.004 319 | 0.000 657 | 0.019 268 |
| 2.26 | −1.401 932 | −1.435 992 | −1.368 641 | | 0.004 135 | 0.000 613 | 0.019 280 |
| 2.28 | −1.406 901 | −1.433 879 | −1.366 458 | | 0.003 959 | 0.000 572 | 0.019 292 |
| 2.30 | −1.411 455 | −1.431 567 | −1.364 087 | | 0.003 793 | 0.000 534 | 0.019 306 |
| 2.32 | −1.415 618 | −1.429 075 | −1.361 552 | | 0.003 635 | 0.000 500 | 0.019 321 |
| 2.34 | −1.419 415 | −1.426 417 | −1.358 874 | | 0.003 486 | 0.000 469 | 0.019 337 |
| 2.36 | −1.422 866 | −1.423 610 | −1.356 071 | | 0.003 345 | 0.000 441 | 0.019 354 |
| 2.38 | −1.425 994 | −1.420 666 | −1.353 161 | | 0.003 212 | 0.000 415 | 0.019 372 |
| 2.40 | −1.428 819 | −1.417 597 | −1.350 158 | | 0.003 086 | 0.000 392 | 0.019 391 |
| 2.42 | −1.431 359 | −1.414 415 | −1.347 075 | | 0.002 968 | 0.000 372 | 0.019 411 |
| 2.46 | −1.435 659 | −1.407 752 | −1.340 709 | | 0.002 752 | 0.000 338 | 0.019 452 |

TABLE I. (*Continued*.)

| | $^3\Pi_g$ potentials[a] | | | | | | |
|---|---|---|---|---|---|---|---|
| $r$ | $E_{11}$(val) | $E_{22}$ (Ryd) | $E_{33}$ (Ryd) | $E_{44}$(val) | $E_{12}$ | $E_{13}$ | $E_{23}$ |
| 2.50 | −1.439 029 | −1.400 746 | −1.334 125 | | 0.002 563 | 0.000 312 | 0.019 497 |
| 2.54 | −1.441 593 | −1.393 456 | −1.327 856 | | 0.002 398 | 0.000 293 | 0.019 544 |
| 2.58 | −1.443 460 | −1.385 935 | −1.320 410 | | 0.002 255 | 0.000 280 | 0.019 592 |
| 2.62 | −1.444 729 | −1.378 225 | −1.313 273 | −1.333 213 | 0.002 132 | 0.000 272 | 0.019 642 |
| 2.64 | −1.445 168 | −1.374 312 | −1.309 625 | −1.341 143 | 0.002 078 | 0.000 270 | 0.019 667 |
| 2.70 | −1.445 819 | −1.362 397 | −1.298 305 | −1.363 557 | 0.001 943 | 0.000 268 | 0.019 744 |
| 2.75 | −1.445 731 | −1.352 328 | −1.288 366 | −1.380 745 | 0.001 857 | 0.000 271 | 0.019 808 |
| 2.80 | −1.445 199 | −1.342 196 | −1.277 896 | −1.396 672 | 0.001 794 | 0.000 278 | 0.019 872 |
| 2.85 | −1.444 327 | | | −1.411 422 | | | |
| 2.90 | −1.443 199 | | | −1.425 071 | | | |
| 2.95 | −1.441 891 | | | −1.437 695 | | | |
| 3.00 | −1.440 463 | | | −1.449 363 | | | |
| 3.05 | −1.438 965 | | | −1.460 141 | | | |
| 3.10 | −1.437 439 | | | −1.470 092 | | | |
| 3.15 | −1.435 918 | | | −1.479 275 | | | |
| 3.20 | −1.434 429 | | | −1.487 745 | | | |
| 3.25 | −1.432 991 | | | −1.495 552 | | | |
| 3.35 | −1.430 323 | | | −1.509 372 | | | |
| 3.45 | −1.427 987 | | | −1.521 084 | | | |
| 3.55 | −1.426 003 | | | −1.530 991 | | | |
| 3.65 | −1.424 358 | | | −1.539 354 | | | |
| 3.80 | −1.422 455 | | | −1.549 477 | | | |
| 4.00 | −1.420 731 | | | | | | |
| 4.20 | −1.419 610 | | | | | | |
| 4.40 | −1.418 807 | | | | | | |
| 4.60 | −1.418 144 | | | | | | |
| 4.80 | −1.417 540 | | | | | | |
| 5.00 | −1.416 980 | | | | | | |
| 5.20 | −1.416 486 | | | | | | |
| 5.40 | −1.416 087 | | | | | | |
| 5.60 | −1.415 801 | | | | | | |
| 6.00 | −1.415 550 | | | | | | |
| 6.50 | −1.415 531 | | | | | | |
| 7.00 | −1.415 366 | | | | | | |
| 7.50 | −1.414 961 | | | | | | |
| 8.00 | −1.414 632 | | | | | | |
| 8.50 | −1.414 610 | | | | | | |
| 9.00 | −1.414 600 | | | | | | |

[a]$E_{14}=E_{24}=0$; $E_{34}=0.0030\ E_h$ for all distances. See text.

results compare favorably with the observed $v=2$ splittings of 84 and 108 $cm^{-1}$ (Ref. 4) and 72 and 106 $cm^{-1}$,[3] so the ECP method[24] provides a suitably accurate description of the spin-orbit interaction.

The calculated vibrational spacings are generally smaller than the measured data, with an average discrepancy of 4% for both the $C\ ^3\Pi_g$ and $d\ ^1\Pi_g$ states (Tables III and IV). Errors of this magnitude can be ascribed primarily to deficiencies in the AO basis employed in the present calculations. Nevertheless, the observed irregularities in the experimental level positions are well described in the present calculations. For example, among the first four measured vibrational levels of the $d\ ^1\Pi_g(3s\sigma)$ state (Table IV), the 2-1 energy difference is the smallest and the 3-2 counterpart the largest, and this highly unusual pattern is also found in the corresponding computed level separations. For the $C\ ^3\Pi_g(3s\sigma)$ state, the agreement between our computed vibrational spacings and the corresponding observed data is somewhat worse (Table III), but it should be noted that thus far there are still relatively large uncertainties in the experimental results themselves.[10]

The salient features of the observed linewidth data[7–11] for the $^{3,1}\Pi_g(3s\sigma)$ states of $O_2$ are also well described in our calculations. For example, only the $v=2$ level of the $^{16}O_2$ $C\ ^3\Pi_g$ state is rotationally resolved of the first five vibrational species. Our calculations predict that the $v=2$ level of the $F_3$ component of the $^3\Pi_g(3s\sigma)$ state has the narrowest linewidth among the $v=0$–4 levels (Table III). The computed values change from 8.8 to 3.1 $cm^{-1}$ when $J$ varies from 2 to 25, which is at least consistent with the measured values given by Sur *et al.*[10] of 6 $cm^{-1}$ and by van der Zande *et al.*[8] of 11 $cm^{-1}$. Sur *et al.*[10] in their REMPI experiment have found that the $v=2$ level gets broader as they scan from 285.8 to 288.3 nm, however. Within a span of 200 $cm^{-1}$ their spectrum goes from rotationally resolved lines of 6 $cm^{-1}$ width in the $F_3$ component to an unresolved

TABLE II. Calculated spin-orbit matrix elements (in $E_h$) between different $x,y$ components of the $^{3,1}\Pi_g$ states of $O_2$ as function of the bond distance $r$ (in $a_0$).

| $r$ | $1\,^3\Pi_g \vert 1\,^3\Pi_g$ | $2\,^3\Pi_g \vert 2\,^3\Pi_g$ | $3\,^3\Pi_g \vert 3\,^3\Pi_g$ | $1\,^1\Pi_g \vert 1\,^3\Pi_g$ | $2\,^1\Pi_g \vert 2\,^3\Pi_g$ | $3\,^1\Pi_g \vert 3\,^3\Pi_g$ |
|---|---|---|---|---|---|---|
| 1.82 | −0.000 382 | 0.000 428 | 0.000 434 | 0.000 371 | 0.000 419 | 0.000 425 |
| 1.86 | −0.000 384 | 0.000 429 | 0.000 434 | 0.000 373 | 0.000 419 | 0.000 424 |
| 1.90 | −0.000 385 | 0.000 428 | 0.000 434 | 0.000 375 | 0.000 418 | 0.000 424 |
| 1.94 | −0.000 386 | 0.000 428 | 0.000 433 | 0.000 376 | 0.000 417 | 0.000 423 |
| 1.98 | −0.000 387 | 0.000 427 | 0.000 432 | 0.000 376 | 0.000 416 | 0.000 421 |
| 2.02 | −0.000 387 | 0.000 426 | 0.000 431 | 0.000 377 | 0.000 415 | 0.000 420 |
| 2.04 | −0.000 387 | 0.000 425 | 0.000 430 | 0.000 377 | 0.000 414 | 0.000 419 |
| 2.06 | −0.000 387 | 0.000 424 | 0.000 429 | 0.000 377 | 0.000 413 | 0.000 418 |
| 2.08 | −0.000 388 | 0.000 423 | 0.000 427 | 0.000 377 | 0.000 412 | 0.000 417 |
| 2.10 | −0.000 387 | 0.000 422 | 0.000 427 | 0.000 377 | 0.000 412 | 0.000 416 |
| 2.14 | −0.000 387 | 0.000 421 | 0.000 425 | 0.000 377 | 0.000 410 | 0.000 414 |
| 2.16 | −0.000 387 | 0.000 420 | 0.000 424 | 0.000 377 | 0.000 409 | 0.000 413 |
| 2.18 | −0.000 387 | 0.000 419 | 0.000 423 | 0.000 377 | 0.000 408 | 0.000 411 |
| 2.20 | −0.000 387 | 0.000 418 | 0.000 421 | 0.000 377 | 0.000 406 | 0.000 410 |
| 2.22 | −0.000 387 | 0.000 417 | 0.000 420 | 0.000 377 | 0.000 405 | 0.000 409 |
| 2.24 | −0.000 387 | 0.000 416 | 0.000 419 | 0.000 377 | 0.000 404 | 0.000 408 |
| 2.26 | −0.000 386 | 0.000 414 | 0.000 418 | 0.000 376 | 0.000 403 | 0.000 407 |
| 2.28 | −0.000 386 | 0.000 413 | 0.000 417 | 0.000 376 | 0.000 401 | 0.000 405 |
| 2.30 | −0.000 386 | 0.000 412 | 0.000 415 | 0.000 376 | 0.000 400 | 0.000 404 |
| 2.32 | −0.000 386 | 0.000 410 | 0.000 414 | 0.000 376 | 0.000 399 | 0.000 402 |
| 2.34 | −0.000 385 | 0.000 409 | 0.000 412 | 0.000 376 | 0.000 397 | 0.000 401 |
| 2.36 | −0.000 385 | 0.000 407 | 0.000 411 | 0.000 375 | 0.000 396 | 0.000 399 |
| 2.38 | −0.000 385 | 0.000 406 | 0.000 409 | 0.000 375 | 0.000 394 | 0.000 398 |
| 2.40 | −0.000 384 | 0.000 404 | 0.000 408 | 0.000 375 | 0.000 393 | 0.000 396 |
| 2.42 | −0.000 384 | 0.000 403 | 0.000 406 | 0.000 374 | 0.000 391 | 0.000 394 |
| 2.46 | −0.000 383 | 0.000 399 | 0.000 403 | 0.000 374 | 0.000 388 | 0.000 391 |
| 2.50 | −0.000 382 | 0.000 396 | 0.000 399 | 0.000 372 | 0.000 384 | 0.000 387 |
| 2.54 | −0.000 380 | 0.000 392 | 0.000 395 | 0.000 372 | 0.000 381 | 0.000 384 |
| 2.58 | −0.000 379 | 0.000 389 | 0.000 392 | 0.000 370 | 0.000 377 | 0.000 380 |
| 2.62 | −0.000 378 | 0.000 385 | 0.000 387 | 0.000 370 | 0.000 374 | 0.000 376 |
| 2.64 | −0.000 377 | 0.000 383 | 0.000 385 | 0.000 369 | 0.000 372 | 0.000 374 |
| 2.70 | −0.000 375 | 0.000 376 | 0.000 379 | 0.000 368 | 0.000 366 | 0.000 368 |
| 2.75 | −0.000 374 | 0.000 371 | 0.000 374 | 0.000 367 | 0.000 360 | 0.000 362 |
| 2.80 | −0.000 372 | 0.000 365 | 0.000 368 | 0.000 365 | 0.000 355 | 0.000 357 |

rotational envelope in the corresponding $F_1$ state.

The present calculations find that in the entire range from $J=2$ to 25 for $v=2$, the linewidth of $F_1$ is larger by a factor of 2 than that of $F_3$. The key to understanding this phenomenon is found in the relative signs of the Rydberg and valence spin-orbit coupling matrix elements. Since the Rydberg $^3\Pi_g(3s\sigma)$ state has only a single $\pi^*$ electron whereas the $\sigma\rightarrow\pi^*$ valence state has three, it is easy to see that this sign must be different in the two cases, as found in the *ab initio* calculations (Table II). As a result, the order of the $F_1$-$F_3$ components is opposite for the valence state ($\Omega=0^+$ lies highest) than for the Rydberg states ($\Omega=0^+$ lies lowest). Consequently, near the crossing of the $(3s\sigma)$ Rydberg and $\sigma\rightarrow\pi^*$ valence $^3\Pi_g$ diabatic potential curves obtained without spin-orbit coupling, the $\Omega=0^+$ ($F_1$ component) of the $C$ state is pushed downward relative to $\Omega=1$, while for $\Omega=2$ ($F_3$ component) the opposite occurs. The crossing point of the corresponding diabatic potential curves obtained with spin-orbit coupling thus occurs at a longer internuclear distance for the $F_1$ component than for $F_3$, thus producing decidedly different mixtures of valence and Rydberg states in their respective spin-perturbed wave functions and hence in their corresponding linewidths.

Recently linewidths of the $v=5$ level of the $C\ ^3\Pi_g$ have been observed,[11] and it was found that their values decrease by a factor of 2 in going from the $F_1$ to the $F_3$ component. The present calculations agree with this finding (Table III), with linewidths of 16.2, 15.6, and 8.1 $cm^{-1}$ having been computed for the $F_1$, $F_2$, and $F_3$ components, respectively, of the $v=5$, $J=2$ level, for example. These results are similar in magnitude to those calculated for $v=2$ (Table III). There is a general tendency for the linewidths to decrease with $J$ in both cases.

For the $^{18}O_2$ isotopomer, the calculations find that the linewidths of the $C$ state $v=4$ rotational levels are sometimes smaller than those of $v=2$ for the same $J,\Omega$ values (Table III). For low $J$ they are much smaller for $v=4$, whereas they become comparable in magnitude for $J\geqslant 20$; the value for the $F_1$ component is lower for $v=4$ for such high $J$ values, whereas the opposite holds for $F_3$ (Table III). Experimentally,[10] an average value of 30 $cm^{-1}$ has been reported for $v=4$ for $^{18}O_2$, compared with 40 $cm^{-1}$ in $v=2$, in at least qualitative agreement with our calculated results.

TABLE III. Calculated and experimental energy positions $T_{vJ}$ (in $cm^{-1}$)[a] and linewidths $\Gamma_{vJ}$ (in $cm^{-1}$) of the spin-split components $F_1$, $F_2$, and $F_3$ for the $v=0-5/J=2-25$ levels of the $C\ ^3\Pi_g(3s\sigma)$ state of $^{16}O_2$. The entries given in a second row (in italics) for $v=2$ and 4, respectively, correspond to the $\Gamma_{vJ}$ of the $^{18}O_2$ isotopomer.

| | Theoretical | | | | | | | | | | | | |
|---|---|---|---|---|---|---|---|---|---|---|---|---|---|
| | $J=2$ | | | $J=10$ | | | $J=20$ | | | $J=25$ | | | |
| $v$ | $F_1$ | $F_2$ | $F_3$ | $F_1$ | $F_2$ | $F_3$ | $F_1$ | $F_2$ | $F_3$ | $F_1$ | $F_2$ | $F_3$ | Expt. |
| | | | | | | $T_{vJ}$ | | | | | | | |
| 0 | −79 | 0 | 97 | −80 | 0 | 97 | −84 | 0 | 100 | −86 | 0 | 101 | 0 |
| 1 | −82 | 1873 | 103 | −83 | 1873 | 104 | −87 | 1871 | 105 | −90 | 1870 | 109 | 1976 [b] |
| 2 | −74 [c] | 1835 | 98 [c] | −76 | 1830 | 99 | −82 | 1816 | 103 | −85 | 1803 | 108 | 1872 [b] |
| 3 | −80 | 1732 | 105 | −80 | 1732 | 107 | −87 | 1735 | 108 | −91 | 1736 | 110 | 1825 [b] |
| 4 | −77 | 1700 | 92 | −78 | 1697 | 97 | −84 | 1683 | 101 | −87 | 1675 | 103 | 1766 [b] |
| 5 | −74 | 1731 | 86 | −77 | 1729 | 98 | −83 | 1722 | 101 | −88 | 1717 | 103 | |
| | | | | | | $\Gamma_{vJ}$ | | | | | | | |
| 0 | 48.0 | 50.5 | 55.4 | 48.9 | 52.0 | 57.2 | 52.0 | 56.0 | 62.2 | 53.5 | 59.0 | 66.2 | 50 [b], 28 [d] |
| 1 | 213 | 210 | 219 | 212 | 213 | 220 | 206 | 212 | 224 | 204 | 214 | 228 | 320 [b], 150 [d] |
| 2 | 17.1 | 13.1 | 8.8 | 15.0 | 10.2 | 7.6 | 9.3 | 7.6 | 4.9 | 6.2 | 3.0 | 3.1 | 6 [b], 11 [d] |
| | *34.2* | *31.0* | *22.0* | *31.3* | *26.0* | *20.2* | *23.0* | *20.0* | *16.0* | *18.5* | *16.5* | *13.0* | *40* [b] |
| 3 | 125 | 120 | 125 | 124 | 117 | 125 | 118 | 118 | 124 | 114 | 116 | 123 | 90 [b] |
| 4 | 21.0 | 26.5 | 32.8 | 22.8 | 28.6 | 35.3 | 28.8 | 34.9 | 43.9 | 33.0 | 40.0 | 48.0 | 60 [b] |
| | *6.4* | *9.6* | *14.8* | *7.6* | *13.2* | *16.5* | *12.0* | *17.0* | *22.0* | *15.0* | *20.0* | *26.5* | *30* [b] |
| 5 | 16.2 | 15.6 | 8.1 | 14.3 | 13.6 | 7.0 | 9.1 | 9.5 | 4.4 | 6.1 | 7.0 | 2.6 | e) |

[a]The calculated energy positions for $F_1(v)$ and $F_3(v)$ are given relative to the corresponding $F_2(v)$ which in turn is given relative to $F_2(v-1)$. $F_2(0)$ is set to zero.
[b]Reference 10.
[c]Experimental results for $F_1$ and $F_3$ are −72 and 106 $cm^{-1}$ (Ref. 3) and −84 and 108 $cm^{-1}$ (Ref. 4), respectively.
[d]Reference 8.
[e]Experimental results for the $F_1$, $F_2$, and $F_3$ components are 3.2, 2.6, and 1.8 $cm^{-1}$, respectively (Ref. 11).

Van der Zande *et al.*[7] observed that the linewidth of the $v=4$ level of the $d\ ^1\Pi_g(3s\sigma)$ state of $^{18}O_2$ becomes narrower as $J$ increases. Our calculations again describe this trend quite well (Table IV), with the $J=1$ value (52.8 $cm^{-1}$) being about twice as large as that for $J=25$. The corresponding measured results are 30 and 15 $cm^{-1}$, respectively. The same authors[7] observed in their translational spectroscopy experiments that for the $v=6$ level intensity is missing in the energy region corresponding to the lower $J$ rotational lines of the $d\ ^1\Pi_g(3s\sigma)$ and the linewidths are smaller than the apparatus resolution. A plausible explanation is that these rotational levels are quite stable to predissociation. Our calculations (Table IV) find that the $v=6$ level of the $^{18}O_2$ $d$ state has a very small linewidth (especially compared to those of $v=5$ and 7) and that it increases with $J$, in good agreement with the observed trends.

Sur *et al.*[9] have measured the $v=0-3$ levels of the $^1\Pi_g(3s\sigma)$ state, and for the $v=0$ level a linewidth of 2 $cm^{-1}$ has been observed. Our calculated values range from 1.3 to 1.5 $cm^{-1}$ between the $J=1$ and 25 (Table IV), in good agreement with the measured result. A rotational analysis has been performed for the $v=0$, 1, 3, and 4 levels of the $d$ state,[7,9] and wide variations in the corresponding rotational constants have been reported. Because of nonadiabatic mixing between the Rydberg and bound valence $^1\Pi_g$ states, the computed spacings between successive rotational levels are often quite irregular in this spectral region, particularly for $v=2$ and 3. To demonstrate this we have computed values for these constants by using the simple formula

$$B_{vJ}=[E(v,J+1)-E(v,J)]/2(J+1), \tag{3}$$

where $E(v,J)$ is the calculated energy for a given rovibrational state. The results are shown in Table V for a number of $v,J$ levels.

The results for $v=0$ and 1 are almost completely independent of $J$, as is normally the case. The corresponding linewidths (Table IV) are found to be relatively small (1–2 $cm^{-1}$), consistent with the fact that a rotational analysis has been successfully made.[9] The $v=0$ $B$ values are 0.02 $cm^{-1}$ smaller than measured,[9] which is consistent with a tendency to overestimate the equilibrium bond lengths of the $O_2$ states in the present treatment. A similar (2%) error is found for the $X\ ^3\Sigma_g^-$ ground state as well, for example. The linewidth of the $v=1$ state is larger than for $v=0$, and the $v=1$ experimental rotational constant is smaller by 0.10 $cm^{-1}$. The increased instability in $v=1$ is an indication of greater mixing with the neighboring $^1\Pi_g$ bound valence state, which in turn leads to a smaller rotational constant by virtue of the longer equilibrium distance of the latter diabatic state (Fig. 1). The present calculated results also show a decrease in going from $v=0$ to $v=1$, but only by 0.03–0.04 $cm^{-1}$ (Table V). It was found that shifting the valence state potential curve up or down by 50 $cm^{-1}$ has very little effect on the computed results. If the original (unshifted) *ab initio* potential curve is employed, however, so

TABLE IV. Calculated and experimental energy positions $T_{vJ}$ (in $cm^{-1}$) and linewidths $\Gamma_{vJ}$ (in $cm^{-1}$) of the $v=0-7/J=1-25$ levels of the $d\ ^1\Pi_g(3s\sigma)$ state of $^{16}O_2$. The entries given in a second row (in italics) for each $v$ correspond to the $\Gamma_{vJ}$ of the $^{18}O_2$ isotopomer.

| | $\Gamma_{vJ}$ | | | | | | | | | | $T_{vJ}$ | |
|---|---|---|---|---|---|---|---|---|---|---|---|---|
| | Theoretical | | | | | Experimental (Refs. 7 and 9) | | | | | Theor. | Expt. |
| $v$ | $J=1$ | 10 | 15 | 20 | 25 | $J=1$ | 10 | 15 | 20 | 25 | ($J=1$) | (Ref. 9) |
| 0 | 1.3 | 1.3 | 1.3 | 1.4 | 1.5 | 2.0 | | | | | 0 | 0 |
| | *1.2* | *1.2* | *1.2* | *1.3* | *1.4* | | | | | | | |
| 1 | 6.4 | 6.1 | 6.1 | 6.1 | 6.4 | a) | | | | | 1791 | 1857 |
| | *6.4* | *5.8* | *5.8* | *5.8* | *5.9* | | | | | | | |
| 2 | 12.0 | 26.0 | 38.0 | 46.8 | | b) | | | | | 3481 | ~3640 |
| | {31.0 | 20.0 | 10.0 | 3.6} [c] | | | | | | | | |
| 3 | 11.0 | 3.6 | 2.6 | | d) | | | | | | 5410 | 5575 |
| | {8.0 | 15.5 | 121.0} [c] | | | | | | | | | |
| 4 | 12.0 | 10.0 | 7.8 | 5.4 | 3.6 | 10 | 10 | <10 | <10 | <10 | 7089 | |
| | *52.8* | *49.0* | *46* | *39.0* | *32* | *30* | *30* | *30* | *20* | *<15* | | |
| 5 | 116 | 115 | 113 | 114 | 106 | 70 | | | | | 8769 | |
| | *109* | *111* | *113* | *115* | *118* | *80* | | | | | | |
| 6 | 34.6 | 37.6 | 40 | 46.2 | 52.0 | <30 | | | | | 10471 | |
| | *4.2* | *5.0* | *6.4* | *8.6* | *12.0* | *≪30* | *≪30* | *<30* | *<30* | *<30* | | |
| 7 | 6.2 | 5.0 | 4.0 | 2.8 | 2.2 | <40 | | | | | 12090 | |
| | *45.0* | *42.0* | *38.5* | *34.0* | *28.0* | *<40* | | | | | | |

[a]Rotationally resolvable up to $J=12$ (Ref. 9).
[b]Rotationally unresolvable (Ref. 9).
[c]Corresponding satellite resonance; see text for details.
[d]Rotationally resolvable up to $J=11$ (Ref. 9).

that the valence state is 1100 $cm^{-1}$ lower than in the present treatment (Table III), a relatively large decrease is observed, producing a value of 1.56 $cm^{-1}$. This result may indicate that the dissociation energy of the bound valence state is too small by roughly 1000 $cm^{-1}$ in the CI calculations, i.e., that more than a constant shift of the valence state potential is required to match the experimental data.

Two distinct spectral features have been observed in the neighborhood of the expected location of the $d\ v=2$ level,[9] separated by about 85 $cm^{-1}$. The corresponding spectral lines are too broad to allow for a rotational analysis. At low temperatures the lower-energy feature has a more compact rotational structure and higher intensity than that of higher energy. As the temperature is increased, the higher-energy feature gains in intensity, however. The present calculations find two resonant vibrational states located in the $v=2$ area, in agreement with these observations. The energy separation between them is 130–150 $cm^{-1}$ for $J=1-25$. It is found that both the linewidth and $B_{vJ}$ values for each of these features vary strongly with $J$. For example, for $J=1$ the calculated linewidth of the low-energy feature is 12.0 $cm^{-1}$, while for $J=20$ it is 46.8 $cm^{-1}$ (Table IV). Corresponding values for the higher-energy feature are 31 $cm^{-1}$ for $J=1$, 20 $cm^{-1}$ for $J=10$, and 3.6 $cm^{-1}$ for $J=20$. These findings are also quite consistent with the above observations. First of all, the computed line broadening is qualitatively in agreement with the fact that neither of the observed spectral features could be rotationally resolved.[9] The variation of the $B_{vJ}$ value with $J$ clearly reflects changes in the ratios of Rydberg/valence $^1\Pi_g$ states in the rovibrational wave functions in this energy region (Fig. 1, Table V). A larger $B_{vJ}$ value means more Rydberg character, which in turn leads to an increase in transition probability between levels of the $d$ and $X\ ^3\Sigma_g^-$ $O_2$ ground state. For $J=1$, the calculated $B_{vJ}$ value of the low-energy $v=2$ feature is thus consistent with the fact that at low temperatures it has much higher intensity. When $J$ is increased the $B_{vJ}$ value of the higher-energy feature increases, so that at $J=10$ it is already larger than that of the lower-energy state. Consequently, at higher temperatures the higher-energy transition gains in intensity so that it eventually becomes stronger than that at lower energy. These results thus mesh quite well with the observed temperature dependence in this region of the $d$-$X$ spectrum.

A rotationally resolved spectral feature has been observed[9] which is located 71 954.80 $cm^{-1}$ above the energy of the $v=0$ level of the $X\ ^3\Sigma_g^-$ ground state of $^{16}O_2$. Its

TABLE V. Calculated and experimental rotational constants $B_{vJ}$ (in $cm^{-1}$) of the $v=0-4/J=1-15$ levels of the $d^1\Pi g(3s\sigma)$ state of $^{16}O_2$. The entries given in a second row (in italics) for $v=2$ and 3 correspond to satellite resonances (see text).

| | Calculated | | | | |
|---|---|---|---|---|---|
| $v$ | $J=1$ | $J=5$ | $J=10$ | $J=15$ | Experimental (Ref. 9) |
| 0 | 1.66 | 1.66 | 1.66 | 1.66 | 1.68 |
| 1 | 1.63 | 1.63 | 1.63 | 1.62 | 1.58 |
| 2 | 1.28 | 1.22 | 1.07 | 0.95 | |
| | *1.19* | *1.23* | *1.37* | *1.48* | |
| 3 | 1.00 | 0.96 | 0.86 | 0.76 | |
| | *0.98* | *1.01* | *1.04* | *0.92* | 1.15 |
| 4 | 1.56 | 1.56 | 1.56 | 1.56 | 1.59 |

rotational constant has been measured to be 1.15 $cm^{-1}$ and has been assigned as the $v=3$ level of the $d\ ^1\Pi_g$ state. By subtracting the $C$-$X$ $T_{00}$ value and the $d$-$C$ energy separation from this energy, one arrives at a $3-0$ $d$ state energy difference of 5575 $cm^{-1}$. The present calculations find two vibrational resonances in this energy region. The one at higher energy has a relatively narrow linewidth and lies 5410 $cm^{-1}$ above the $d$ $v=0$ level (Table IV). It seems clear that this state should be assigned to the observed $v=3$ level at 5575 $cm^{-1}$, so there is an underestimation in the present calculations of 165 $cm^{-1}$ or 3%. As shown in Table V the $B_{vJ}$ value for this state varies sharply with $J$, reaching a maximum at $J=10$ of 1.04 $cm^{-1}$. This value is still 0.11 $cm^{-1}$ smaller than that reported experimentally, but it is considerably smaller than those reported for $v=0$ and 1 and thus fits in with the observed pattern quite well. The discrepancy is probably caused in the main by inaccuracies in the long-distance portion of the valence $^1\Pi_g$ state, as already mentioned.

The calculated energy separation between the $v=3$ level and the lower-energy resonance is about 170 $cm^{-1}$ on average for different $J$ values. For $J=1$ the two rovibrational states have about the same $B_{vJ}$ value (Table V), but as $J$ increases, that of the lower-energy state decreases sharply (0.86 $cm^{-1}$ at $J=10$ and 0.76 $cm^{-1}$ at $J=15$). As discussed above for the $v=2$ level, a small $B_{vJ}$ value is indicative of relatively little Rydberg character in the rovibrational wave function, and hence a small Franck–Condon factor for transitions from $X\ ^3\Sigma_g^-$. This state of affairs explains at least partially why thus far no low-energy feature near the $v=3$ level has been observed experimentally.

Moving on to the $v=4$ level, it is found that its $B_{vJ}$ value no longer varies with $J$. At 1.56 $cm^{-1}$, the computed value is again about 2% smaller than measured (Table V). It is comparable to that observed for $v=1$, but still notably smaller than for $v=0$, so some mixing between the Rydberg and bound valence $^1\Pi_g$ diabatic states is still indicated. The $d$ $v=4$ level is located above the dissociation limit of the valence $^1\Pi_g$ state, so perturbations from it come mainly from its inner limb.

The competition between radial and spin-orbit effects on the predissociation of the $v=0-2$ levels of the $d\ ^1\Pi_g(3s\sigma)$ state has been studied by van der Zande *et al.*[8] using translational spectroscopy. They concluded that the $v=0$ level is predissociated via a spin-orbit interaction with the $^3\Pi_g(3s\sigma)$ state, whereas the $v=2$ level decays via a homogeneous mechanism involving the bound $^1\Pi_g$ valence state (see Fig. 1). The $v=1$ state represents an intermediate case in this respect. The present calculations find the predissociation linewidths caused by the homogeneous interaction to be $10^{-4}$, 1.0, and 9.6 $cm^{-1}$, respectively, for the $v=0$, 1, and 2 levels ($J=1$), i.e., by setting the spin-orbit interaction between the $^3\Pi_g(3s\sigma)$ and $^1\Pi_g(3s\sigma)$ states to zero. When both the homogeneous and spin-orbit interaction are included, the computed linewidths change to 1.3, 6.4, and 12.0 $cm^{-1}$ (Table IV, $J=1$). Hence, our calculations are qualitatively in accord with the observations made by van der Zande *et al.*[8]

Finally, we have investigated the effects of rotational couplings ($S$-uncoupling[33]) on the linewidths of the $^3\Pi_g$ $(3s\sigma)$ states. It was found that in the low-$J$ case the effects of rotational-electronic coupling are negligible, but for high $J$ the effects of this interaction become apparent. For example, for the $v=2$, $J=1$ level of the $C\ ^3\Pi_g(3s\sigma)$ state, the computed linewidths are nearly the same with or without including the $S$-uncoupling, but for $J=20$ the computed $F_1$-$F_3$ linewidths are 10.4, 7.0, and 4.0 $cm^{-1}$ if the rotational coupling is neglected, whereas values of 9.4, 7.5, and 4.8 $cm^{-1}$ are obtained when it is included (Table IV).

## IV. CONCLUSION

An *ab initio* CI treatment for the $^{3,1}\Pi_g$ manifold of excited states has been employed to study the effect of Rydberg-valence mixing on the properties of the associated rovibrational states. A diabatic transformation succeeds in providing a clear separation into Rydberg and valence electronic states and helps to simplify the analysis of the computed results. Three types of electronic couplings are considered: spin-orbit, radial, and rotational. The rovibrational basis consists of 200 Hermite polynomials for each of 13 $\Omega$ electronic states. The complex scaling technique is then employed to obtain rovibrational energies and linewidths, with special emphasis on the results for the $d\ ^1\Pi_g$ and $C\ ^3\Pi_g\ 3s\sigma$ states. To obtain the best agreement with available experimental data, particularly for the linewidth results, it is desirable to shift the $^1\Pi_g$ bound valence state's potential curve upward by 1100 $cm^{-1}$ so that the observed energy separation between the $C$ $v=0$ level and the $^1D+{}^1D$ atomic asymptote is reproduced, but also to displace it toward smaller $r$ values by 0.038 $a_0$ so that its crossing point with the $d\ ^1\Pi_g$ potential curve is unchanged. A smaller displacement is also applied to the $^3\Pi_g$ valence energy but all other potential curves and coupling elements are taken directly from the *ab initio* CI calculations.

The present treatment is able to account for a large number of trends in the measured linewidths, energy locations, and rotational constants of the $C,d\ ^{3,1}\Pi_g$ vibrational levels. Both the $d$-$C$ and $C$-$X$ energy splittings are also well described in the calculations. Of the lowest $C\ ^3\Pi_g$ levels $v=2$ has the narrowest linewidth for $^{16}O_2$ and $v=4$ for $^{18}O_2$, in agreement with the experimental findings. The $F_1$ $\Omega$ component is found to have about twice the linewidth as that of $F_3$, also as observed, and it is shown that the explanation lies in the different $\pi^*$ occupation numbers in the Rydberg $\pi^*\rightarrow 3s\sigma$ and valence $\sigma\rightarrow\pi^*$ states. The spin-orbit splittings among the three triplet components are obtained accurately through the use of effective core potentials. Rotational coupling is found to have noticeable effects for high-$J$ values of the $C$ $v=2$ state. Moreover, the $v=5$ linewidth is found to be comparable to that of $v=2$ and there is a general tendency for the instability to decrease with $J$.

The most interesting effects are found for the $d\ ^1\Pi_g$ state, however. They are predominantly caused by its interaction with the $^3\Pi_g$ valence state at low $v$ and with the bound $^1\Pi_g$ valence state at higher energy. The irregular

spacing observed among the $v=0-3$ levels is reproduced in the present calculations. The spin-orbit coupling mechanism is shown to dominate in the predissociation of the $v=0$ level, whereas radial coupling with the $^1\Pi_g$ valence state is much more important for $v=2$, as observed by van der Zande *et al.*[8] The strongest Rydberg-valence mixing occurs for the $v=2$ and 3 levels. In both cases nearby spectral features are computed which have a larger contribution from the valence $^1\Pi_g$ than for the $\pi^* \rightarrow 3s\sigma$ Rydberg diabatic state. The corresponding linewidths are notably larger than for the levels in the $d$-state manifold itself, consistent with their composition. Only the $v=2$ satellite feature has been observed, and so it seems clear that the corresponding $v=3$ feature is too broad to be resolved in the experiments carried out to date. It is shown that there is a strong correlation between the magnitudes of the linewidths and rotational constants of the $d$-state rovibrational levels. The observed variations in the $B$ values of the $v=0$, 1, 3, and 4 levels of the $d$ state are reproduced almost quantitatively in the calculations. A large decrease is found for both $v=2$ and $v=3$ relative to the more typical value expected for a pure Rydberg state. The $v=2$ portion of the spectrum could not be rotationally resolved, in agreement with the computed linewidth results. Finally, the temperature dependence of the two features observed near the expected $v=2$ location can be understood on the basis of the computed linewidth variations with $J$ in each case.

## ACKNOWLEDGMENTS

The authors wish to express their gratitude to Professor Per Jensen and Dr. Aleksey B. Alekseyev for numerous helpful discussions during the course of this work. This work was supported in part by the Deutsche Forschungsgemeinschaft in the form of a Forschergruppe grant. The financial support of the Fonds der Chemischen Industrie is also hereby gratefully acknowledged. I.D.P. is a Fellow of the Alexander von Humboldt Foundation and is grateful for its financial support.

[1] T. A. York and J. Comer, J. Phys. B **16**, 3627 (1983).
[2] A. Sur, C. V. Ramana, and S. D. Colson, J. Chem. Phys. **83**, 904 (1985).
[3] A. Sur, C. V. Ramana, W. A. Chupka, and S. D. Colson, J. Chem. Phys. **84**, 69 (1986).
[4] S. Katsumata, K. Sato, Y. Achiba, and K. Kimura, J. Electron Spectrosc. **41**, 325 (1986).
[5] R. D. Johnson, G. R. Long, and J. W. Hudgens, J. Chem. Phys. **87**, 1977 (1987).
[6] W. J. van der Zande, W. Koot, J. R. Peterson, and J. Los, Chem. Phys. Lett. **140**, 175 (1987).
[7] W. J. van der Zande, W. Koot, and J. Los, J. Chem. Phys. **89**, 6758 (1988).
[8] W. J. van der Zande, W. Koot, and J. Los, J. Chem. Phys. **91**, 4597 (1989).
[9] A. Sur, R. S. Friedman, and P. J. Miller, J. Chem. Phys. **94**, 1705 (1991).
[10] A. Sur, L. Nguyen, and N. Nikoi, J. Chem. Phys. **96**, 6791 (1992).
[11] R. A. Copeland, private communation.
[12] R. S. Friedman and A. Dalgarno, J. Chem. Phys. **90**, 7606 (1989).
[13] R. S. Friedman and A. Dalgarno, J. Chem. Phys. **93**, 2370 (1990).
[14] R. S. Friedman, M. L. Du, and A. Dalgarno, J. Chem. Phys. **93**, 2375 (1990).
[15] Y. Li, M. Honigmann, G. Hirsch, and R. J. Buenker, Chem. Phys. Lett. **212**, 185 (1993).
[16] R. P. Saxon and B. Liu, J. Chem. Phys. **67**, 5432 (1977).
[17] R. P. Saxon and B. Liu, J. Chem. Phys. **73**, 870 (1980).
[18] R. P. Saxon and B. Liu, J. Chem. Phys. **73**, 876 (1980).
[19] M. Honigmann, R. J. Buenker, G. Hirsch, and S. Schöttke, J. Phys. B **25**, 389 (1992).
[20] Y. Li, M. Honigmann, K. Bhanuprakash, G. Hirsch, R. J. Buenker, M. A. Dillon, and M. Kimura, J. Chem. Phys. **96**, 8314 (1992).
[21] E. Balslev and J. M. Combes, Commun. Math. Phys. **22**, 280 (1971).
[22] N. Moiseyev, Int. J. Quantum Chem. **20**, 835 (1981).
[23] C. M. McCurdy, in *Autoionization/Recent Developments and Applications*, edited by A. Temkim (Plenum, New York, 1985), p. 135.
[24] L. F. Pacios and P. A. Christiansen, J. Chem. Phys. **82**, 2664 (1985).
[25] T. H. Dunning, Jr. and P. J. Hay, in *Methods of Electronic Structure Theory*, edited by H. F. Schaefer III (Plenum, New York, 1977), p. 1.
[26] R. J. Buenker and S. D. Peyerimhoff, Theor. Chim. Acta **35**, 33 (1974).
[27] R. J. Buenker and S. D. Peyerimhoff, Theor. Chim. Acta **39**, 217 (1975).
[28] R. J. Buenker, Int. J. Quantum Chem. **29**, 435 (1986).
[29] S. Krebs and R. J. Buenker, J. Chem. Phys. **103**, 5613 (1995).
[30] R. J. Buenker, in *Proceedings of Workshop on Quantum Chemistry and Molecular Physics in Wollongong, Australia*, edited by P. Burton (University Press, Wollongong, 1980); in *Studies in Physical and Theoretical Chemistry*, Vol. 21, Current Aspects of Quantum Chemistry, edited by R. Carbó (Elsevier, Amsterdam, 1981), p. 17; R. J. Buenker and R. A. Phillips, J. Mol. Struct. Theochem. **123**, 291 (1985).
[31] E. R. Davidson, in *The World of Quantum Chemistry*, edited by R. Daudel and B. Pullman (Reidel, Dordrecht, 1974), p. 17.
[32] G. Hirsch, P. J. Bruna, S. D. Peyerimhoff, and R. J. Buenker, Chem. Phys. Lett. **52**, 442 (1977); D. B. Knowles, J. R. Alvarez-Collado, G. Hirsch, and R. J. Buenker, J. Chem. Phys. **92**, 585 (1990).
[33] H. Lefebvre-Brion and R. W. Field, *Perturbations in the Spectra of Diatomic Molecules* (Academic, Orlando, 1986), p. 39.